Gram, R. E. Mischke, and J. Arvieux, to be published.
[2]Yu. A. Batusov, S. A. Bunyatov, V. M. Sidorov, and V. A. Yarba, Joint Institute for Nuclear Research, Dubna, Report No. JINR P-1474, 1963 (unpublished), and Yad. Fiz. 3, 309 (1966) [Sov. J. Nucl. Phys. 3, 223 (1966)].
[3]L. Gilly, M. Jean, R. Meunier, M. Spighel, J.-P. Stroot, P. Duteil, and A. Rode, Phys. Lett. 11, 224 (1964).
[4]P. E. Boynton, T. Devlin, J. Solomon, and V. Perez-Mendez, Phys. Rev. 174, 1083 (1968).
[5]C. J. Cook, M. E. Nordberg, Jr., and R. L. Burman, Phys. Rev. 174, 1374 (1968).
[6]R. L. Burman, M. P. Baker, M. D. Cooper, R. H. Heffner, D. M. Lee, R. P. Redwine, J. E. Spencer, T. Marks, D. J. Malbrough, B. M. Preedom, R. J. Holt, and B. Zeidman, Phys. Rev. C 17, 1774 (1978).
[7]K. K. Seth, H. Nann, S. Iverson, M. Kaletka, J. Hird, and H. A. Thiessen, Phys. Rev. Lett. 41, 1589 (1978).
[8]K. K. Seth, S. Iverson, H. Nann, M. Kaletka, J. Hird, and H. A. Thiessen, Phys. Rev. Lett. 43, 1574 (1979).
[9]J. Davis, J. Källne, J. S. McCarthy, R. C. Minehart, C. L. Morris, H. A. Thiessen, G. Blanpied, G. R. Burleson, K. Boyer, W. Cottingame, C. F. Moore, and C. A. Goulding, Phys. Rev. C 20, 1946 (1979).
[10]J.-P. Albanèse *et al.*, Nucl. Instrum. Methods 158, 363 (1978).
[11]Yu. A. Batusov, S. A. Bunyatov, N. Dalkhazhav, G. Ionice, E. Losnyanu, V. Mihul, V. M. Sidorov, D. Tuvdendorzh, and V. A. Yarba, Yad. Fiz. 9, 378 (1969) [Sov. J. Nucl. Phys. 9, 221 (1969)].
[12]C. W. Bjork, S. E. Jones, T. R. King, D. M. Manley, A. T. Oyer, G. A. Rebka, Jr., J. B. Walter, R. Carawon, P. A. M. Gram, F. T. Shivley, C. A. Bordner, and E. L. Lomon, Phys. Rev. Lett. 44, 62 (1980).
[13]These values differ from the preliminary results presented by Ingram (Ref. 1) because of momentum-dependent corrections.
[14]J. Mougey, M. Bernheim, D. Royer, D. Tarnowski, S. Turck, P. D. Zimmerman, J. M. Finn, S. Frullani, D. B. Isabelle, G. P. Capitani, E. De Sanctis, and I. Sick, Phys. Rev. Lett. 41, 1645 (1978).
[15]M. Thies, Y. Horikawa, and F. Lenz, private communication; M. Thies, Schweizerisches Institut für Nuklearforschung Report No. 79-007, 1979 (unpublished).

Evidence for Nuclear Superfluidity in ^{236}U Isomeric- and Prompt-Fission Modes

Carlos A. Fontenla and Doracy P. Fontenla
Brookhaven National Laboratory, Upton, New York 11973
(Received 16 August 1979)

Isomer fission in ^{236m}U, $t_{1/2}=125$ nsec, from ^{235}U(d,pf) was compared with prompt fission ^{235}U(n_{th},f), in twin experiments. Fine structure in the total kinetic energy, average total kinetic energy as a function of mass, and mass yield were observed in isomer fission of ^{236m}U. This observation is compatible with a superfluid descent from saddle to scission points. Two peaks in the total-kinetic-energy distribution from isomer fission are observed near fragment mass 132, and this is interpreted as due to the proton-pairing effect at $Z=50$.

PACS numbers: 28.85.Ge, 27.90.+b

Isomer fission tunneling from the ground state of the second well, in a double-humped fission barrier, proceeds with several megaelectronvolts less in initial excitation energy E^* (around 4 MeV less for ^{236m}U, Ref. 1) than thermal-neutron–induced fission of the same nucleus. Isomer fission studies therefore provide a unique opportunity to test, in nuclei of low fissility parameter Z^2/A, the behavior attributed to shell and pairing effects over a wide range of fission fragment masses. How this behavior changes with E^* has been studied at energies at and above the fission barrier. Study of isomer fission extends the range of energies E^* below the fission barrier where the relative importance of shell and pairing effects can change. In particular, if superfluidity plays a role in fission, these effects should arise or be enhanced with decreasing E^*.

In the present work fine structure has been observed for isomer fission of ^{236m}U in the total kinetic energy $E_K{}^m$ and in the mass yield spectra as well as in the average total kinetic energy $\langle E_K{}^m(\mu)\rangle$ as a function of fragment mass μ. The same quantities obtained in a twin experiment for prompt thermal-neutron–induced fission of ^{235}U do not show this structure. When only those events are selected which correspond to a heavy fragment mass near $\mu=132$ amu, then the $E_K{}^m$ isomer spectrum has the striking feature of being split in two resolved peaks. This is an effect not previously observed in fission which may have significant implications.

Isomeric fission of ^{236}U was studied with the ^{235}U$(d,p)^{236m}$U reaction at the Brookhaven National Laboratory (BNL) tandem Van de Graaff facility. The data presented here were obtained mostly at $E_d = 11$ MeV with some runs at $E_d = 12$ MeV. The average deuteron current on the target was 1.5 μA.

The recoil technique was used to separate isomeric-fission events from prompt-fission events at the target. Isomeric ^{236m}U leaves the target with the momentum transferred in the (d,p) reaction and fissions in flight with $T_{1/2} = 125$ nsec half-life. In flight, isomeric fission fragments were detected in coincidence by two 4-cm^2 Si surface-barrier detectors positioned at 15° relative to the beam and carefully collimated so that they could not see the target directly. A third detector looking directly at the target was used as a deuteron-induced prompt-fission monitor.

The prompt neutron-induced fission ^{235}U(n_{th},f) experiment was carried out in a collimated thermal beam at the BNL high-flux–beam reactor. The same geometry, collimators, detectors, ^{252}Cf calibration source, and electronic equipment were used as for isomer fission.

Two inherent differences that still remain were minimized and considered in the comparison: First, in-flight isomer fission fragments do not have target material (U) or backing (C foils) to go through as prompt-fission fragments do. This effect was minimized in prompt fission with use of very thin targets and backings. A 5-μg/cm^2 C + 1-μg/cm^2 ^{235}U (99.75% enriched) two-foil sandwich target was used and the proper correction for energy absorption was applied. Second, in the isomer-fission experiment, there is a low-energy background produced by fast neutrons (due to deuteron stripping) reaching the solid-state detectors. The background was minimized by restricting the counting geometry and also decreasing the beam energy. The probability of pulse pileup with fission fragment pulses was measured by superimposing the signal from a precision pulser during a period of counting time; less than 0.5% was obtained.

From the directly measured kinetic energies in a double energy experiment, the so-called provisional masses μ are obtained.[2] Figure 1(b) shows the prompt and isomer provisional mass yield distributions. The average value of the isomer peak is shifted 0.7 amu to higher asymmetry than the prompt peak and a pronounced fine structure appears. The fine-structure peaks, especially the more asymmetric one at $\mu = 143$ are near the shoulders in the prompt mass distributions. Both yields are normalized and the shift of the average, to larger asymmetry in isomer fission, seems to be due to different ratios among the fine-structure peaks. The two at $\mu = 136$ and $\mu = 139$ appear with a reduced yield in favor of an increase in the more asymmetric one ($\mu = 143$), when compared with prompt fission. It can be concluded that the isomer mass distribution of ^{236}U favors asymmetry when compared with prompt thermal-neutron–induced fission.

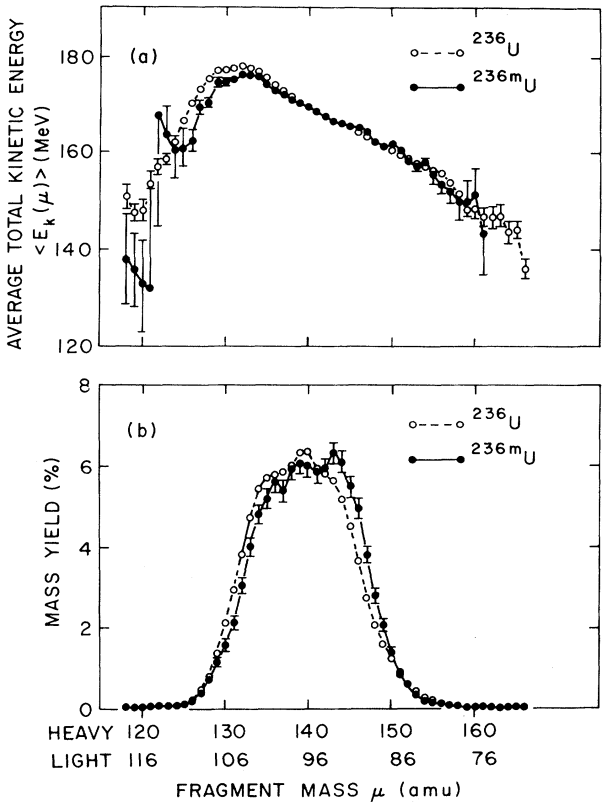

FIG. 1. Results for ^{236m}U isomer fission and ^{236}U prompt fission. (a) Average post-neutron-evaporation total kinetic energy as a function of provisional mass μ. (b) Normalized provisional mass yield distribution. For clarity the upper or lower part of some error bars has been omitted.

The heights of the first and second barriers of the ^{236}U double-humped fission barrier, extracted from model calculations, are 6.1 and 5.8 MeV, respectively.[1] If the properties of the mass distributions are defined at the saddle point, the prompt-fission mass yield distribution will reflect mostly the properties of the first saddle point. Isomeric fission arising from tunneling from the ground state of the second well through the second barrier will show only the properties of the second saddle point. A second saddle un-

stable to asymmetric distortions has been theoretically obtained[3,4,5] with a static potential-energy surface. A different theoretical approach is used by Hooshyar and Malik[6] in which an isomer mass distribution with some similarity to Fig. 1(b) was predicted. Static scission-point models[7,8] have obtained qualitative agreement with the observed general trend of mass, charge, and kinetic-energy distributions.

The influence of dynamics in the last stage of fission with a superfluid[9,10] nuclear-matter motion was proposed[11] as the explanation for the observed[12] fine structure in the prompt-fission mass yield and average total kinetic energy as a function of mass of ^{229}Th(n_{th},f) and in the spontaneous-fission mass yield of ^{248}Cm. Fine structure in the mass yield was interpreted[11] as a preference for double-even mass division with preservation of the pairing configuration in a superfluid descent from saddle to scission points. Fine structure in partial spectra of the mass yield of ^{235}U(n_{th},f) when high values of fragment kinetic energy are selected has been observed.[13,14] One revealing result here is that by reducing the E^* (comparing prompt and isomer fission in the same nucleus) the effect is sufficiently enhanced to be seen in the total mass spectrum. In Fig. 1(a) the average total kinetic energy $\langle E_K(\mu)\rangle$ for each mass division is plotted. It can be seen in this figure that isomer fission presents a fine structure not observed in prompt fission. Fine structure in $\langle E_K(\mu)\rangle$ has been interpreted[11] as a result of the energetically favored double-even mass division.

From $\mu \simeq 155$ to $\mu \simeq 134$ the values of $\langle E_K(\mu)\rangle$ in Fig. 1(a) are essentially the same in both cases, in spite of the fact that prompt fission starts the descent toward scission from ≈ 4 MeV higher than isomer fission. This difference can be explained by excitation of internal degrees, higher fragment deformation, or different charge split. About 0.4 MeV of this difference can be accounted for by the fact that the measured energies are post neutron evaporation if prompt fission finally releases the difference in E^* as a higher average number of evaporated neutrons. Excitation of internal degrees can be associated with a viscous descent, from saddle to scission points, in prompt fission, compared with a superfluid descent in isomer fission. If we approach the interval around $\mu \simeq 132$ (doubly magic $N=82$, $Z=50$), in Fig. 1(a), part of the difference in E^* now appears as kinetic energy, with prompt fission having 2–3 MeV higher kinetic energy. This indicates the onset of a region of comparable pairing effect for prompt and isomer fission. The pairing gap increases[10,15] with decreasing E^*. It is known that for mass 132 the average number of evaporated neutrons as a function of mass has a deep minimum (almost no neutrons are evaporated) in prompt fission (and this can be expected to be valid also in isomer fission). This implies for mass 132 the lowest excitation of internal degrees (coldest fission fragment) and minimum deformation. The average total number of evaporated neutrons is also minimum for the mass split 132/104.

In Fig. 2 the total-kinetic-energy distribution has been split in two mass intervals. The total kinetic energy distribution for all masses has the

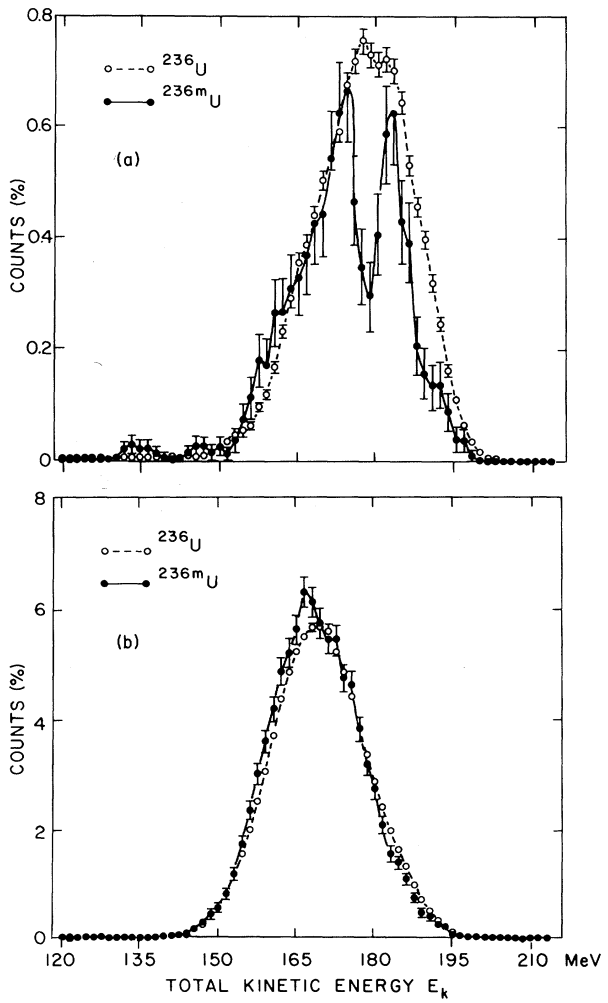

FIG. 2. The normalized post-neutron-evaporation total-kinetic-energy distribution for all provisional masses in ^{236m}U isomer fission and ^{236}U prompt fission, split in two intervals: (a) for masses $\mu = 118$–133 amu, (b) for masses $\mu = 134$–166 amu.

average total kinetic energy $\langle E_K \rangle$, 1.2 MeV higher for prompt fission. Isomer-fission fine-structure peaks in Fig. 2(b) can be associated with the peaks in the mass distribution.

The behavior in Fig. 1(a) changes approaching $\mu \simeq 132$, and it can be seen in Fig. 2(a) that the total kinetic energy $E_K{}^m$ for isomer fission is split in two peaks for this region. Almost all the counts in the peaks of Fig. 2(a) come from masses 133 to 129. Both peak positions are maintained through the interval and the spectra for each mass were added to increase the statistics. The relative height of the two peaks changes through the interval, the low-energy one increasing from 133 to 129.

The high-energy peak in Fig. 2(a) can indicate and be the consequence of the persistence through the mass interval of the closed shell $Z = 50$ (with $Z = 42$ in the complementary fragment), due to the proton pairing effect. For low E^* fission the following observations suggest a reluctance of the charge $Z = 50$ to be split: (1) the persistence of the peaks through several mass units observed in this work; (2) the low yield[16] of x rays attributed to charge $Z = 49$ (and to the complementary charge) for $^{236}_{92}$U, $^{240}_{94}$Pu, and $^{252}_{98}$Cf fission; (3) the increase[12,17] in mass yield and kinetic energy at symmetry for $^{255}_{99}$Es and $^{256}_{100}$Fm fission for which $Z = 50$ does not need to be broken at mass symmetry; and (4) the very asymmetric charge distribution[18] for fission-fragment mass 104 with suppression of the charge $Z = 43$ in ^{236}U. This effect is expected to be enhanced for isomer fission, with the lower E^* favoring superfluidity.

The low-energy peak in Fig. 2(a) can be a result of breaking the closed shell $Z = 50$ with an increased softness toward deformation and a substantial total-kinetic-energy decrease as a consequence. An alternative explanation is that the low-energy peak is originated by neutron transfer during the descent toward scission. An initially asymmetric mass configuration with homogeneous charge density, will shift the mass split toward mass symmetry (without change in the charge asymmetry) if a large fluctuation in neutrons transferred toward the light fragment occurs. These events will have a large charge deviation from the most probable events that have approximately equal charge density in both fragments. A large fluctuation in neutrons transferred toward the heavy fragment will produce the opposite effect. A coherent neutron transfer instead of diffusion can be expected in a superfluid state.[19]

If we compare, for the isomer-fission fine-structure peaks, Fig. 2(a) with 2(b) we can see similarity in their structure. The low-energy peak at 174 MeV in Fig. 2(a) in the context of the previous explanation results as an extension to more symmetric masses by neutron transfer (toward the light fragment) of charge splits associated with the energy peaks noticed in Fig. 2(b) around this energy value. Conversely, the high-energy peak at 183 MeV in Fig. 2(a) extends by neutron transfer (toward the heavy fragment) to more asymmetric mass split and appears as a modulation in the high-energy part of Fig. 2(b).

We would like to acknowledge the help received at different stages of this work from P. Thieberger, E. der Mateosian, W. Kane, and P. Bond. We thank Professor R. C. Leite for his encouragement and support during our leave of absence from the Universidade Estadual de Campinas.

This work was performed under the auspices of the U. S. Department of Energy and was also supported by Universidade Estadual de Campinas, Fundação de Amparo è Pesquisa do Estado de São Paulo (FAPESP) and Conselho Nacional de Desenvolvimento Cientffico e Technológico (CNPq), Brasil.

[1]B. B. Back, J. P. Bondorf, G. A. Otroschenko, J. Pedersen, and B. Rasmussen, Nucl. Phys. A165, 449 (1971).

[2]H. W. Schmitt, J. H. Neiler, and F. J. Walter, Phys. Rev. 141, 1146 (1966).

[3]P. Möller and S. G. Nilsson, Phys. Lett. 31B, 283 (1970).

[4]M. Bolsterli, E. O. Fiset, J. R. Nix, and J. L. Norton, Phys. Rev. C 5, 1050 (1972).

[5]M. Brack, J. Damgaard, A. S. Jensen, H. C. Pauli, V. M. Strutinsky, and C. Y. Wong, Rev. Mod. Phys. 44, 320 (1972).

[6]M. A. Hooshyar and F. B. Malik, Phys. Lett. 38B, 495 (1972).

[7]F. Dickmann and K. Dietrich, Nucl. Phys. A129, 241 (1969).

[8]B. D. Wilkins, E. P. Steinberg, and R. R. Chasman, Phys. Rev. C 14, 1832 (1976).

[9]A. Bohr, B. R. Mottelson, and D. Pines, Phys. Rev. 110, 936 (1958).

[10]J. J. Griffin, Phys. Rev. 132, 2204 (1963).

[11]S. Bjørnholm, Phys. Scr. 10A, 110 (1974).

[12]J. P. Unik, J. E. Glinder, L. E. Glendenin, K. F. Flynn, A. Gorski, R. K. Sjoblom, in *Proceedings of the Third IAEA Symposium on the Physics and Chemistry of Fission, Rochester, New York, 1973* (IAEA, Vienna, 1974), Vol. 2, p. 19.

[13]T. D. Thomas and R. Vandenbosch, Phys. Rev. 133B, 976 (1964).

[14]W. N. Reisdorf, J. P. Unik, and L. E. Glendenin, Nucl. Phys. A205, 348 (1973).
[15]L. G. Moretto, Phys. Lett. 40B, 1 (1972).
[16]W. Reisdorf, J. P. Unik, H. C. Griffin, and L. E. Glendenin, Nucl. Phys. A177, 337 (1971).
[17]R. C. Ragaini, E. K. Hulet, R. W. Loughęed, and J. Wild, Phys. Rev. C 9, 339 (1974).
[18]H. G. Clerc, K. H. Schmidt, H. Wohlfarth, W. Lang, H. Schrader, K. E. Pferdekämper, R. Jungmann, M. Asghar, J. P. Bocquet, and G. Siegert, Nucl. Phys. A247, 74 (1975).
[19]M. Gaudin, Nucl. Phys. A144, 191 (1970).

Determination of Limiting Angular Momenta for Fusion from Statistical-Model Fits to Mass Distributions of Evaporation Residues

S. Kox, A. J. Cole, and R. Ost
Institut des Sciences Nucléaires, 38026 Grenoble Cedex, France
(Received 28 November 1979)

Improved statistical-model calculations allow a search for the lower and upper limiting angular momenta of compound-nucleus formation that give best fits to evaporation-residue mass distributions. For the $^{16}O+^{16}O$ reaction in the energy range $E_{lab}=35-80$ MeV, optimal fits are obtained for low-l cutoff 0, and maximum l equal to l_{cr}, obtained from total fusion cross sections.

PACS numbers: 25.70.Bc, 25.70.Hi

The decay of the compound nucleus is well understood in terms of a statistical evaporation model. The fusion reaction leading to compound-nucleus formation, on the other hand, is a highly complex process whose theoretical description always requires simplifying assumptions. A basic question is which impact parameters (partial waves l) lead to fusion. The maximum l value (l_{cr}) determines the maximum possible so-called critical angular momentum J_{cr} of the compound nucleus. l_{cr} can be calculated[1] from the total fusion cross section $[\sigma_{fusion}=\pi\lambda\!\!\!^{-2}(l_{cr}+1)^2]$ if we assume that the probability of compound-nucleus formation is unity for all incoming partial waves between 0 and l_{cr}. A cutoff for low l values is predicted, however, by recent time-dependent Hartree-Fock calculations[2] and discussed in experimental publications.[1,3]

One way to gain information on limiting l values is to perform statistical-model calculations for J distributions and to choose the correct distribution by the best fit to the data. Unfortunately, useful calculations are time consuming and require large amounts of computer storage. Most calculations that are found in the literature are therefore one-shot calculations that use a distribution between $J=0$ and $J=l_{cr}$ with l_{cr} as determined from total fusion cross sections. The interpretation of differences between experiment and theory remains rather speculative. We report here on a method that permits the choice of the best statistical-model fit from a large number of calculations with different initial angular momentum distributions of the compound nucleus.

In this Letter we concentrate our investigation on the compound system $^{16}O+^{16}O$, where extensive data are reported[3] for energies $E_{lab}=35-80$ MeV. Less intensive studies on other compound systems with $A\leq 32$ where there are experimental data available[1,4,5] seem to confirm the results reported here.

The statistical-model calculations were carried out using the Monte Carlo computer code LANCELOT.[5,6] Relative probabilities for competing decay modes from a parent nucleus with excitation energy E_x and angular momentum J_I are calculated using the Hauser-Feshbach formula[7] which, for emission of a particle b of spin j removing orbital angular momentum l and kinetic energy ϵ, may be written

$$P^{J_I,E_x}(b,l,\epsilon) = T_l(\epsilon)\sum_{S=|J_I-l|}^{J_I+l}\sum_{J_f=|S-j|}^{S+j}\rho(E_f,J_f). \quad (1)$$

Here $T_l(\epsilon)$ is a transmission coefficient obtained, with the parabolic barrier approximation,[8] from optical-model potentials and $\rho(E_f,J_f)$ is the density of states in the daughter nucleus which at low energies is obtained from experimentally observed levels, and at higher energies is the Lang[9] Fermi-gas density with parameters obtained